Use of integral-equation theory in determining the structure and thermodynamics of liquid alkali metals

J. L. Bretonnet and N. Jakse
Laboratoire de Physique des Liquides et des Interfaces, Institut de Physique, Université de Metz, Metz Cedex 3, France
(Received 11 January 1994)

Assuming that the interionic forces can be modeled by the effective pair potential $u(r)$ arising in second-order pseudopotential theory, we have calculated the structure factor $S(q)$ and some thermodynamic properties of the alkali metals. The pair potential is derived from a local empty-core pseudopotential including a core-valence exchange correlation. The calculations of the structure and thermodynamics are performed with the self-consistent integral equation called the hybridized mean spherical approximation (HMSA). The results presented in detail are in very good agreement with experiments for all the alkali metals near their melting points as well as for Rb and Cs along the liquid-vapor coexistence curve.

I. INTRODUCTION

Over the last decade, thermodynamic perturbation theories based on the hard-sphere reference system have obtained real success in the calculation of the structure factor of liquid metals (Kumaravadivel and Evans,[1] McLaughlin and Young,[2] Kahl and Hafner,[3] Bretonnet and Regnaut[4]). Meanwhile, attempts have been made to develop new integral equations. In the earliest semianalytic theories such as the Yvon-Born-Green, the Percus-Yevick, and the hypernetted-chain (HNC), the pair-correlation function was only a weak functional dependence of the structural properties on the pair potential so that substantial differences in pair potential often provided modest changes in the structure factor. With the modified HNC (MHNC) and variational modified HNC (VMHNC) the liquid-state theory has reached a high level of accuracy over a large extend of the region of stability (Rosenfeld and Ashcroft,[5] Matsuda *et al.*,[6] Gonzalez, Gonzalez, and Silbert,[7] Chen and Lai[8]). An alternative procedure is to achieve thermodynamic consistency of the virial and compressibility equations of state by interpolating between two standard integral equations (Rogers and Young,[9] Zerah and Hansen,[10] Kahl[11]).

In this paper, we present our results of the thermodynamics and the structure of the alkali metals, using such an interpolation procedure between the soft-core mean spherical approximation (SMSA) and the HNC, called the hybridized mean spherical approximation (HMSA), by means of a switching constant chosen to force thermodynamic self-consistency. It is found that the HMSA results are close to the SMSA, confirming that the SMSA is one of the most appropriate standard equations for realistic metallic interactions (Madden and Rice,[12] Jakse and Bretonnet[13]). Taking advantage of the absence of adjustable parameter in the SMSA we also proceed to study the response of the calculated structure factor to variation of the cutoff distance of the pair potential.

The contents of the paper are the following. In Sec. II, mention is made of the local pseudopotentials as well as the effective pair potential used and the HMSA. In order to calculate the pair potential we use a pseudopotential well adapted for alkali metals, for which the essential feature is the departure from Coulombic behavior beyond the core radius. We also briefly present the technical procedure used to solve the nonlinear integral equations, which is no longer time consuming since the development of efficient algorithms. In Sec. III we discuss the results of the structure factor and some thermodynamic properties for all alkali metals as well as the structure factor of Rb at density close to the critical point, where the electron-ion interaction becomes less amenable to a pseudopotential description. Finally, we examine the role of the attractive part of the pair potential on the structure factor of Cs.

II. THEORY

A. Pseudopotential and effective pair potential

In the pseudopotential perturbation theory the pair potential is expressed under the standard form

$$u(r)=\frac{1}{8\pi^3}\int d^3q\frac{4\pi Z^2e^2}{q^2}[1-F_N(q)]e^{iq\cdot r}\ , \tag{1}$$

where Z is the valence and $F_N(q)$ is the normalized energy-wave-number characteristic defined as

$$F_N(q)=\left[\frac{q^2}{4\pi Ze^2}\right]^2\left[1-\frac{1}{\epsilon(q)}\right]\left[\frac{1}{1-G(q)}\right]w^2(q)\ . \tag{2}$$

The expression for $F_N(q)$ is dependent only on the scattering momentum q through the Hartree dielectric function $\epsilon(q)$, the local-field correction $G(q)$ and the form factor, $w(q)$, of the pseudopotential. To study the effects of exchange and correlation on the structure factor we employ the two well-known local-field corrections of Vashishta-Singwi[14] and Ichimaru-Utsumi.[15] For Li, we use the Hoshino and Young[16] pseudopotential modified by Das and Joarder[17] to reduce some of the drawbacks of the model. The interested reader should

refer to their original papers for mathematical details. For the other alkali metals, we employ the new local generalized empty-core (GEC) pseudopotential proposed by Hasegawa *et al.*[18] The essential feature of this pseudopotential is the inclusion of the core-valence exchange correlation for which the tail of the electron-ion interaction deviates slightly of the Coulombic form. The departure is hardly distinguishable for Na but becomes substantial for heavy alkali metals such as Rb and Cs. The GEC pseudopotential is defined as

$$v(r)=\begin{cases}0 & \text{if } r<R_c\ , \\ -\dfrac{Ze^2}{r}[1+a\exp(-br)] & \text{if } r>R_c\ ,\end{cases} \tag{3}$$

where a and b are determined so that the pseudopotential fits the potential calculated in the local-density-functional approximation. They are tabulated by Hasegawa *et al.*[18] for a large number of elements. One practical merit of the GEC pseudopotential is to have only R_c as fixed parameter. The second advantage is to procure a simple analytic expression for the unscreened form factor, namely,

$$w(q)=-\frac{4\pi Ze^2}{q^2}\cos(qR_c) \times\left\{1+\frac{\pi q^2}{b^2+q^2}\left[1+\frac{b}{q}\tan(qR_c)\right]\exp(-bR_c)\right\}\ . \tag{4}$$

With the effective pair potential known, integral equations are able to provide us the liquid structure for alkali metals.

B. Integral equations

The pair-correlation function $g(r)$ of a classical fluid interacting through a pair potential, $u(r)$, is determined from the solution of the Ornstein-Zernike (OZ) relation

$$g(r)-1-c(r)=\rho\int d^3r'[g(r')-1]c(|\mathbf{r}-\mathbf{r}'|) \equiv\gamma(r)\ , \tag{5}$$

where $c(r)$ is the direct correlation function and ρ is the number density. The OZ relation must be supplemented by a closure approximation which, in our case, is that of Zerah and Hansen:[10]

$$g^{\mathrm{HMSA}}(r)=\exp(-\beta u_1(r)) \times\left\{1+\frac{\exp[f_0\{\gamma(r)-\beta u_2(r)\}]-1}{f_0}\right\}, \tag{6}$$

where $\beta(=1/k_BT)$. The effective pair potential $u(r)$ is split, according to the scheme of Weeks, Chandler, and Anderson,[19] into its sharp short-range repulsive part, $u_1(r)$, and its weak long-range attractive part, $u_2(r)$:

$$u_1(r)=\begin{cases}u(r)-u(r_0) & \text{if } r<r_0\ , \\ 0 & \text{if } r>r_0\ ,\end{cases}$$
$$u_2(r)=\begin{cases}u(r_0) & \text{if } r<r_0\ , \\ u(r) & \text{if } r>r_0\ .\end{cases} \tag{7}$$

r_0 is the position of the principal minimum of $u(r)$. This separation is particularly convenient to examine the role of the different parts of $u(r)$ that determine the structure factor of metallic liquids. f_0 is a mixing function, which presents under various forms (Zerah and Hansen,[10] Lai, Wang, and Tosi,[20] Kahl[11]), chosen to force the thermodynamic self-consistency (TSC). Equation (6) has two limiting cases according to the value of the mixing parameter f_0, namely SMSA when $f_0=0$ and HNC when $f_0=1$. Between these two limits, the interpolation is carried out by the variation of the parameter f_0. Our choice of f_0 is motivated by the fact that the interpolation takes place in a quite narrow region of $g(r)$ and it is very convenient to observe the degree of contribution of the two standard equations involved (Bretonnet and Jakse).[21] The interpolation is performed to achieve the thermodynamic self-consistency by requiring the equality between the relation arising from the compressibility route in the grand-canonical ensemble [see for example Egelstaff[22]], on one hand, which is the inverse long-wavelength limit of the structure factor $S(q)$:

$$\beta\frac{\partial P}{\partial\rho}\bigg|_T=1-4\pi\rho\int c(r)r^2dr=\frac{1}{S(0)} \tag{8}$$

and that coming from the virial equation of state, on the other hand,

$$\beta\frac{\partial P}{\partial\rho}\bigg|_T=\beta\frac{\partial}{\partial\rho}(\beta^{-1}\rho+P_0+P'_{i-i}+P''_{i-i})_T\ , \tag{9}$$

where the number density ρ is related to the electronic density n by $\rho=nZ$, Z being the valence. The different contributions to the pressure P are explicitly defined as in the paper of Hasegawa and Watabe:[23]

$$P_0=\rho^2\frac{\partial U_0(\rho)}{\partial\rho}\ , \tag{10}$$

$$P'_{i-i}=-\frac{2\pi\rho^2}{3}\int\frac{r^3\partial u(r;\rho)}{\partial r}g(r;\rho)dr\ , \tag{11}$$

$$P''_{i-i}=2\pi\rho^2\int r^2\frac{\rho\partial u(r;\rho)}{\partial\rho}g(r;\rho)dr\ . \tag{12}$$

While $u(r;\rho)$ is the effective pair potential given by Eq. (1), the term $U_0(n)$ contains all the different volume-dependent contributions to the total energy per ion of the metal, $E/\langle N\rangle$, derived by Finnis[24]

$$U_0(\rho)=E_{\mathrm{eg}}-\rho^{-1}B_{\mathrm{eg}}+\phi(r=0)\ , \tag{13}$$

where E_{eg} and B_{eg} are the energy of the homogeneous electron gas and the bulk modulus of the free-electron gas, respectively, and $\phi(r=0)$ is one half the electrostatic interaction between an ion and its surrounding cloud

$$\phi(r=0)=-\frac{Z^2e^2}{\pi}\int_0^\infty F_N(q)dq\ . \tag{14}$$

Practically, the free parameter of the local pseudopotential (R_0 for Li and R_c for the other alkali metals) is fitted to obtain numerically the experimental value of the long-wavelength limit of the structure factor. Simultaneously, f_0 is chosen to give the equality between Eqs. (8)

and (9). Consequently the TSC is achieved at the observed $S(0)$. However, the use of pseudopotential theory to obtain the pair potential leads to an electronic inconsistency (Brovman and Kagan[25]). As a result, the virial pressure, calculated from the total energy, does not vanish and the two equations of state cannot be fully consistent. To avoid this problem, the zero-pressure condition is forced in Eq. (9) to get a full TSC.

C. A summary of the LMV method

One of the most attractive numerical procedure for solving Ornstein-Zernike equation is based upon an advantageous combination of the Newton-Raphson and the successive substitution methods, originally proposed by Gillan.[26] Labik, Malijevsky, and Vonka[27] (LMV) employed a similar but several times more rapid, procedure using a sine function basis set instead of Gillan's roof functions. Following LMV, it is suitable to define the functions

$$\Gamma(r)=r\gamma(r) , \tag{15}$$

$$C(r)=rc(r) , \tag{16}$$

as well as their explicit Fourier transforms in the discrete form

$$\Gamma(r_i)=\frac{\Delta q}{2\pi^2}\sum_{j=1}^{N-1}\tilde{\Gamma}(q_j)\sin\left[\frac{\pi}{N}r_i q_j\right];\quad i=1,\ldots,N-1 , \tag{17}$$

$$\tilde{C}(q_j)=4\pi\Delta r\sum_{i=1}^{N-1}C(r_i)\sin\left[\frac{\pi}{N}r_i q_j\right];\quad j=1,\ldots,N-1 , \tag{18}$$

where Δq $[=\pi/(N\Delta r)]$ is the grid mesh in reciprocal space. The Fourier transform of the Ornstein-Zernike equation [Eq. (5)] and the closure relation [Eq. (6)] may now be written in terms of the new functions as

$$\tilde{\Gamma}(q_j)=\frac{\rho\tilde{C}^2(q_j)}{q_j-\rho\tilde{C}(q_j)} \tag{19}$$

and

$$F[\Gamma(r_i)]=r_i\exp(-\beta u_1(r_i))\times\left\{1+\frac{\exp[f_0[\Gamma(r_i)/r_i-\beta u_2(r_i)]]-1}{f_0}\right\}-\Gamma(r_i)-r_i . \tag{20}$$

The algorithm developed by LMV consists in solving the nonlinear set of Eq. (19) for the first M Fourier components using the Newton-Raphson (NR) method, while the high-order components ($j>M$) are obtained by direct iterations. In order to bring the NR scheme into play, $\tilde{C}(q_j)$ are approximated by a first-order expansion around the initial estimates $\tilde{\Gamma}^{(0)}(q_j)$, namely,

$$\tilde{C}(q_j)=\tilde{C}^{(0)}(q_j)+\sum_{k=1}^{N-1}\tilde{C}_{j,k}[\tilde{\Gamma}(q_k)-\tilde{\Gamma}^{(0)}(q_k)] , \tag{21}$$

where the coefficients are defined as

$$\tilde{C}_{j,k}=\frac{2}{N}\sum_{i=1}^{N-1}\left.\frac{dF}{d\Gamma(r_i)}\right|_{\Gamma=\Gamma_i^{(0)}}\times\sin\left[\frac{\pi}{N}r_i q_k\right]\sin\left[\frac{\pi}{N}r_i q_j\right] . \tag{22}$$

The NR method applied to Eq. (19) leads to the following set of linear equations:

$$\sum_{k=1}^{M}J_{j,k}\Delta\tilde{\Gamma}(q_k)=\frac{\rho\tilde{C}^2(q_j)}{q_j-\rho\tilde{C}(q_j)}-\tilde{\Gamma}(q_j);\ j=1,\ldots,M , \tag{23}$$

where $J_{j,k}$ is the Jacobian matrix elements

$$J_{j,k}=\delta_{jk}-\frac{\rho\tilde{C}(q_j)}{q_j-\rho\tilde{C}(q_j)}\times\left[2+\frac{\rho\tilde{C}(q_j)}{q_j-\rho\tilde{C}(q_j)}\right]\tilde{C}_{j,k};\ j=1,\ldots,M . \tag{24}$$

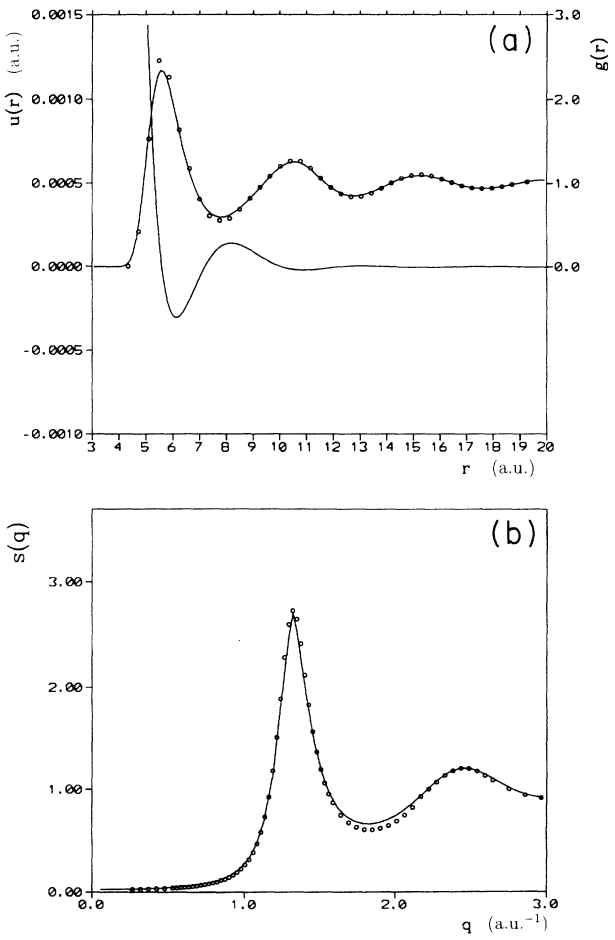

FIG. 1. (a) Effective pair potential $u(r)$ and pair-distribution function $g(r)$ of liquid Li (b) Structure factor of liquid Li; [empty dots: experimental data of Waseda (Ref. 30)].

TABLE I. Input data: temperature T, electronic radius r_s, pseudopotential parameters R_c, a, b, R_0, β, and the TSC parameter f_0.

	Li	Na	K	Rb	Cs
T (K)	463	378	343	313	303
r_s (a.u.)	3.311	4.047	5.022	5.405	5.783
R_c (a.u.)		2.02	2.61	2.95	3.26
a		10	20	21	22
b		2	1.7	1.4	1.2
R_0 (a.u.)	0.47				
β	25.6				
f_0	0.10	0.64	0.42	0.33	0.15

As the right-hand side of Eq. (23) is known, the set of linear equations can be solved for the unknown difference $\Delta\tilde{\Gamma}(q_k)$ between the previous solution of $\tilde{\Gamma}(q_k)$ and its new one in the iterative procedure, which subsequently yields a correct $\tilde{\Gamma}(q_k)$. The procedure is then repeated until the convergence is achieved and the correct correlation functions are obtained. Even if the solution is not exact, since the Jacobian is expanded to the first order only, the efficiency of the method is very good. It depends on the number M of equations involved in the NR method, but the final correlation functions are not. If $M=N$ we are faced to a very large system of linear equations time consuming whereas $M=1$ corresponds to the direct iteration method very slowly convergent when it does. For the Lennard-Jones potential we had chosen M between 15 and 30 with $N=1024$ (Bretonnet and Jakse[21]). The results presented below are obtained with M currently situated around 60.

III. RESULTS AND DISCUSSION

A. The structure factor

Table I lists the values of the input data entering the calculations, as well as those of the mixing parameter f_0 obtained with the procedure detailed in Sec. II B. In Figs. 1(a)–5(b) we show $g(r)$ and $S(q)$ calculated by the HMSA with the local-field correction of Ichimaru and Utsumi.[15] Our results of $S(q)$ are compared with the accurate measurements of Huijben and van der Lugt[28] for Na, K, and Cs as well as those of Copley and Rowe[29] for

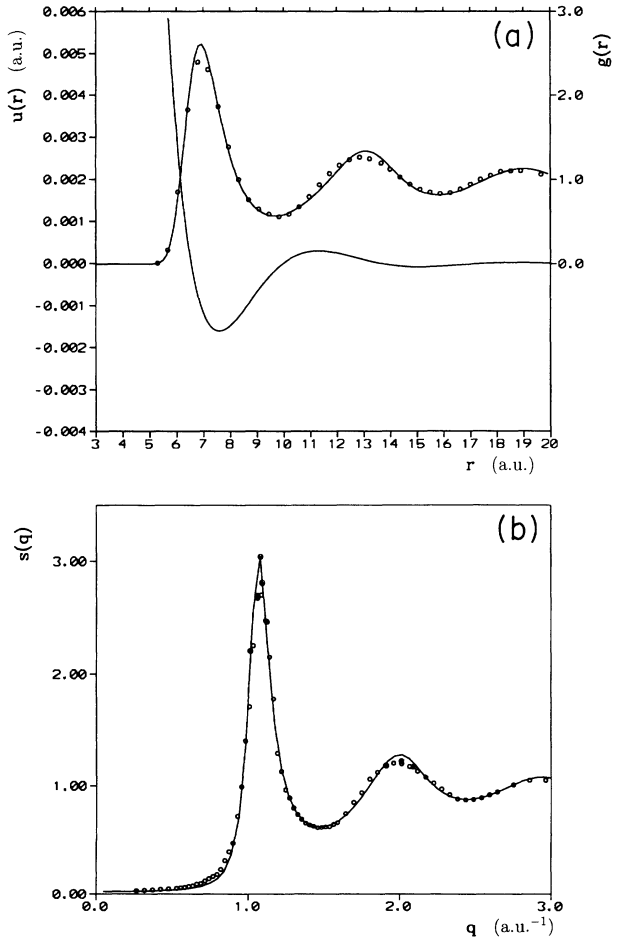

FIG. 2. (a) same as in Fig. 1(a) for Na, (b) same as in Fig. 1(b), for Na [full dots: experimental data of Huijben and van der Lugt (Ref. 28)].

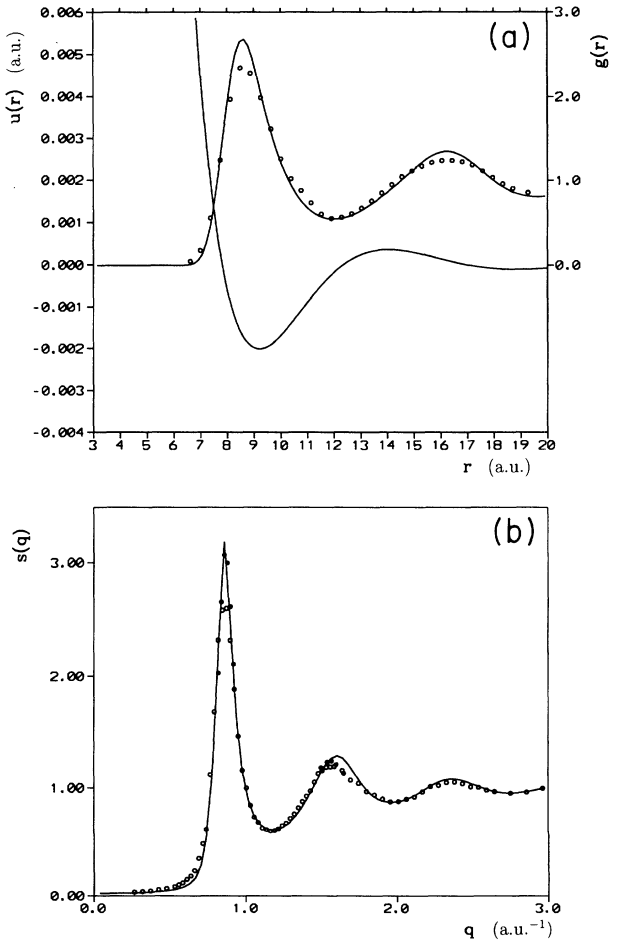

FIG. 3. (a) same as in Fig. 1(a), for K, (b) same as in Fig. 1(b), for K (full dots: experimental data of Huijben and van der Lugt, Ref. 28).

Rb. For the sake of comparison, we also have reported those of Waseda[30] for $S(q)$ and $g(r)$. On the scale of the figures, the curves are indistinguishable except in the range of the first peak of $S(q)$. The theoretical results of $S(q)$ agree quite well with the experiments particularly for small q, since R_c has been fitted on experimental $S(0)$ of Ruppersberg and Speicher[31] for Li and those of Webber and Stephens[32] for the other elements. It is also interesting to observe that for K, the second peak of $S(q)$ goes slightly towards the large-q region whereas for Cs it is shifted towards the low-q region. For Li, Na, and Rb the second peak of $S(q)$ has excellent position with respect to the experiment.

It is worth mentioning that the results for Na, K, Rb, and Cs are comparable to those of Chen and Lai[8] who used the VMHNC and a nonlocal pseudopotential. The pair potential described in this paper has also been used by Matsuda *et al.*[6] to perform the calculations of the structure factor with molecular-dynamics simulation. The results obtained by these authors are in excellent agreement with the experimental structure factor of alkali metals. We therefore tested the accuracy and efficiency of the HMSA method to experiments in order to spare computer time.

If the calculations are performed with the Vashishta and Singwi[14] dielectric function, the pair-correlation function is hardly affected though the pair potential is quite sensitive to it. Also, no discrepancy is visible between the curves of the structure factor as a consequence of the used procedure, which consists of fitting the theoretical long-wavelength limit to the experimental $S(0)$.

Incidentally, we explore the influence of the two parameters a and b of the Hasegawa *et al.*[18] pseudopotential by changing their values arbitrarily. The roles of a and b are, roughly speaking, opposite and the inspection of Figs. 6(a) and 7(a) shows that their effects on the pair potential extend only a small distance outside the core region. The increase of b — or the reduction of a — causes the displacement of the short-range repulsive part of $u(r)$ towards larger distances and the reduction of the width of the attractive well. Consequently, the ions have a

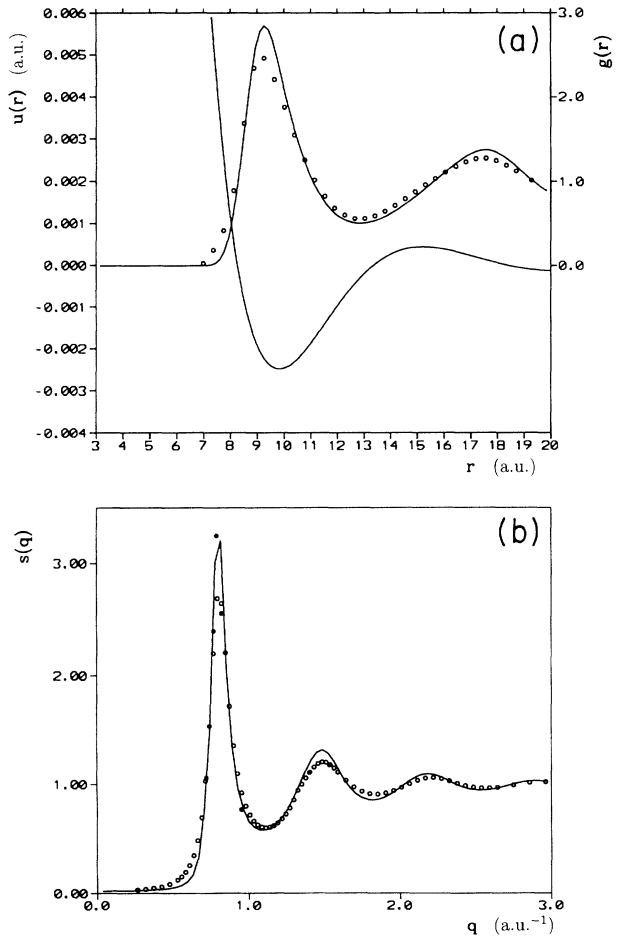

FIG. 4. (a) same as in Fig. 1(a), for Rb, (b) same as in Fig. 1(b), for Rb (full dots: experimental data of Copley and Rowe, Ref. 29).

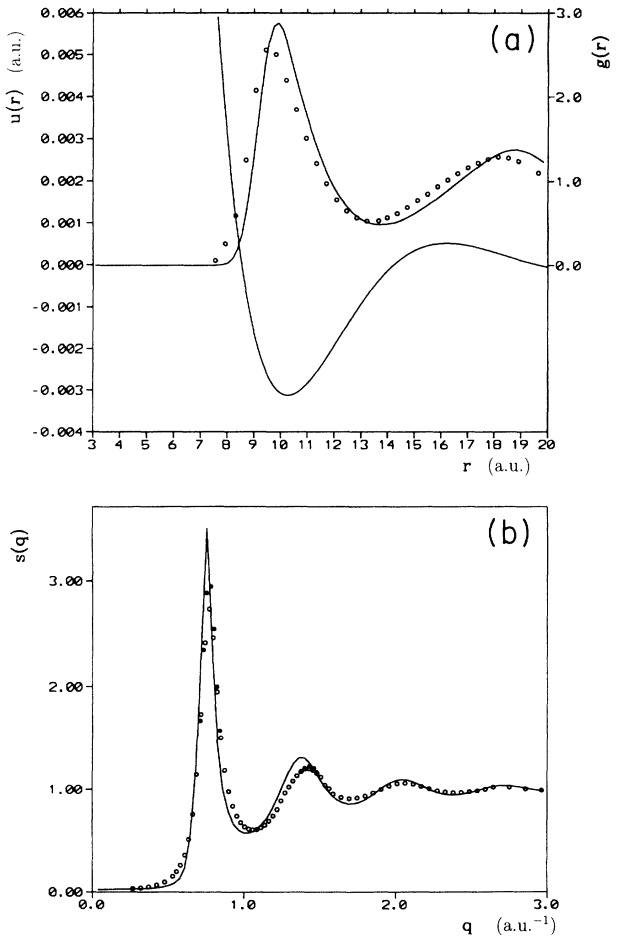

FIG. 5. (a) same as in Fig. 1(a), for Cs, (b) same as in Fig. 1(b), for Cs (full dots: experimental data of Huijben and van der Lugt, Ref. 28).

stronger tendency to cluster in the vicinity of the first minimum of $u(r)$ and the main peak of $g(r)$ becomes higher. At the same time, the peaks of $S(q)$ undergo an enhancement and the oscillations are slightly shifted towards smaller values of q [Figs. 6(b) and 7(b)].

In Table I, we can see that, with the exception of Na, the TSC values of f_0 are below 0.5. It shows that SMSA is much better adapted for the calculation of the structure factor of alkali metals than HNC. According to the argument of Chihara,[33] the SMSA integral equation might become less accurate at lower densities, but also increasingly accurate at higher temperatures when the attractive well of $u(r)$ becomes more and more shallow. It is of interest therefore, to compare the structure factor of Rb with the experiments, near its critical point to test the model at high temperature and low density. A detailed discussion of the low-q behavior of $S(q)$, for Rb and Cs, is given by Jakse and Bretonnet.[13] Comparing $g(r)$ and $S(q)$ of Rb just before the metal-nonmetal transition happens, the results agree very well with the experimental data of Franz *et al.*[34] and Winter *et al.*[35] In particular, the position of the first maximum of $S(q)$ does not change when the critical point is approached, while its height becomes lower and its width broader.

In spite of the numerous theoretical calculations of the structure factor for liquid metals to know which regions of $S(q)$ contain information about the repulsive and the oscillatory parts of $u(r)$, it still seems difficult to separate the structural effects attributable to the repulsive part from those attributable to other features in the pair potential. To examine these effects, some attention has been focused on the influence of the cutoff distance of the pair potential on $g(r)$ and $S(q)$. We have performed our calculations with the SMSA ($f_0=0$) that is particularly well adapted for it. The results of $g(r)$ and $S(q)$ are shown, in Figs. 8(a) and 8(b), for Cs at 1373 K in order to be compared with those of Matsuda, Hoshino, and Watabe,[36] who analyzed this problem in determining the structure factor of liquid Cs with the MHNC approximation. Although our procedure of cutting is somewhat different we can observe the same results as these authors. The truncation of $u(r)$ at its first minimum (r_0) decreases the

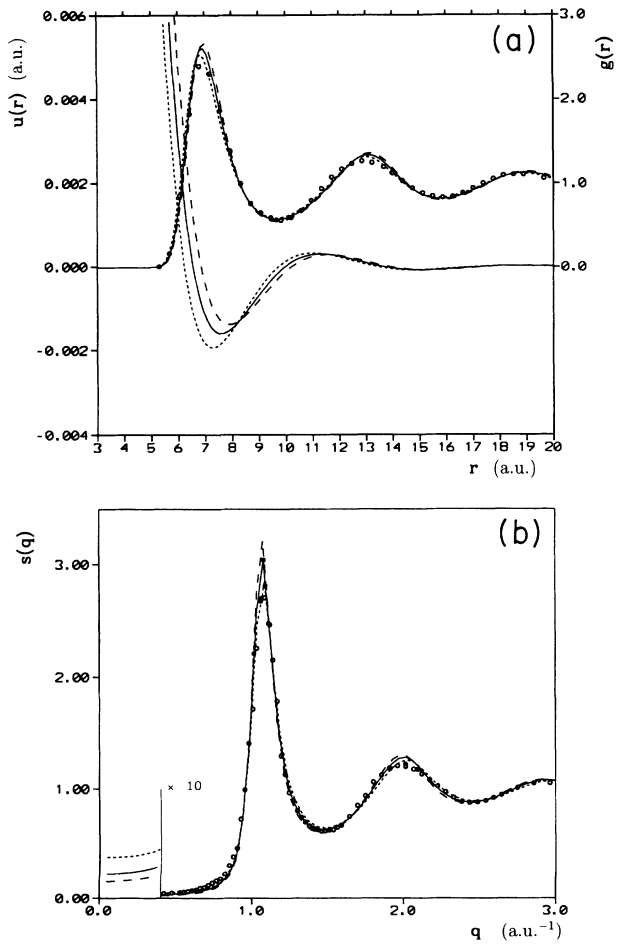

FIG. 6. Influence of the pseudopotential parameter a. (a) Effective pair potential and pair-distribution function of liquid Na, at 378 K. (b) Structure factor of liquid Na, at 378 K. $a=2$: ———, $a=10$: ——, $a=18$: — — —.

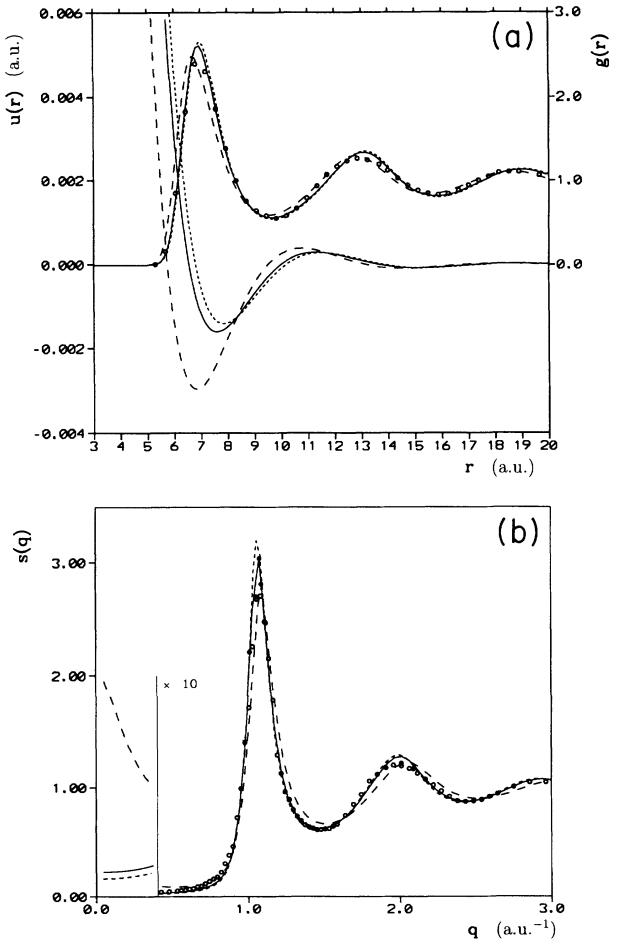

FIG. 7. Influence of the pseudopotential parameter b. (a) Effective pair potential and pair-distribution function of liquid Na, at 378 K. (b) Structure factor of liquid Na, at 378 K. $b=1.6$: ———, $b=2$: ——, $b=2.4$: — — —.

TABLE II. Contributions to the internal energy $E/\langle N\rangle$ given in 10^{-3} a.u. and compared to the experimental values E_{exp} of Gschneidner (Ref. 37).

	E_{id}	E_{eg}	$-\rho^{-1}B_{eg}$	$\phi(r=0;\rho)$	E_{str}	$E/\langle N\rangle$	E_{exp}
Li	2.20	−76.65	−21.96	−164.86	2.91	−258.36	−259.00
Na	1.80	−81.53	−9.21	−136.96	−1.69	−227.59	−232.00
K	1.63	−79.87	−1.14	−113.79	−4.38	−197.55	−195.60
Rb	1.49	−78.26	0.68	−106.87	−5.04	−188.00	−187.00
Cs	1.44	−76.45	2.05	−101.47	−5.61	−180.04	−175.70

magnitude of the first peak of $g(r)$ and causes the subsequent peaks to be strongly damped when they are compared to the correct $g(r)$ given by the full curve of $u(r)$. For the structure factor, the main peak is much lower than that of the correct $S(q)$ and the long-wavelength limit reaches its lowest value; the same remark can be made for Rb. Then, if $u(r)$ is truncated at the following nodes (r_1 and r_2), the oscillations of $g(r)$ and $S(q)$ become slightly enhanced but the long-wavelength limit lies either over the correct $S(0)$ for the cutoff distance r_1 or below for r_2. The behavior of $S(0)$ for the next cutoff distances, which is not presented in the figure for clarity, converges on the correct values of $S(0)$. An interesting feature can be seen when $u(r)$ is cut off at its first maximum (r_1') because $g(r)$ is shifted upwards the correct $g(r)$ and goes slowly to unity at large distances. This unexpected behavior has also been observed by Matsuda, Hoshino, and Watabe, who suggest that it might be related to a metastable supercooled state. From these observations we conclude that the effect of the long-range attractive part of $u(r)$ is to increase the amplitude of the oscillations in $g(r)$ and $S(q)$ without changing their positions and the cutoff distance determines drastically the behavior of the structure factor for small values of q.

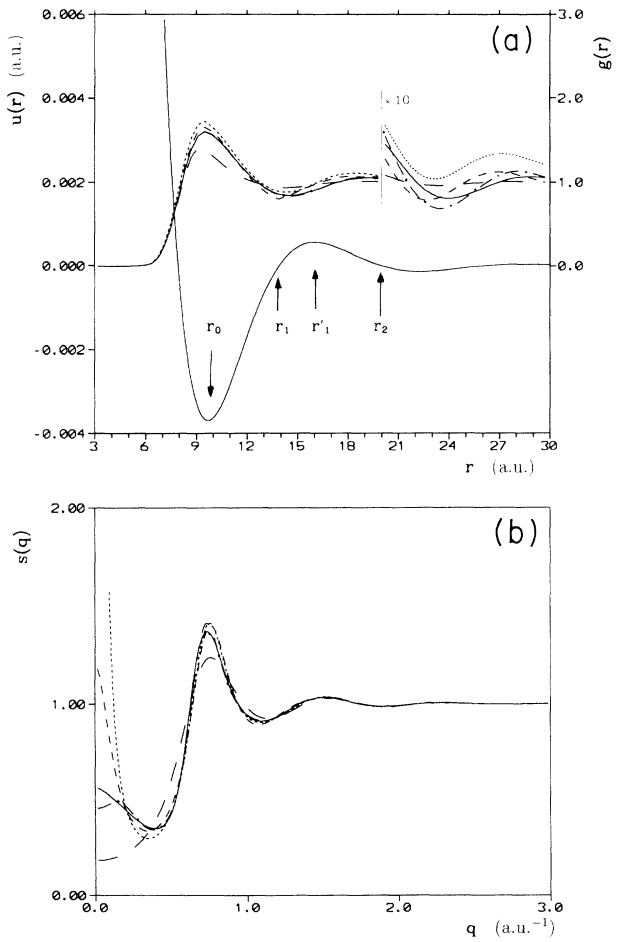

FIG. 8. Influence of the cutoff distance of $u(r)$. (a) Effective pair potential and pair-distribution function of liquid Cs, at 1373 K. (b) Structure factor of liquid Cs, at 1373 K. The full curves are obtained with the total effective potential and the others are obtained with the cutoff distances r_0: ———, r_1: — — —, r_2: —·—·— ——, r_1': · · · ·.

B. The thermodynamic properties

We now return to the calculations of the energy, pressure and bulk modulus that are necessary to perform the TSC. The internal energy

$$\frac{E}{\langle N\rangle}=E_{id}+U_0(\rho)+E_{str}\ , \tag{25}$$

where $U_0(\rho)$ is determined as stated in Sec. II B, is compared with the experimental values of Gschneidner[37] in Table II. As expected, the most important contribution comes from the self-energy volume term, $\phi(r=0)$, which increases when we go from light to heavy alkali metals. In contrast, the ideal term $E_{id}=3\beta^{-1}/2$ and the structural term $E_{str}=(1/2N)\sum_{i\neq j}u(r_{ij};\rho)$ always keep moderated values.

The various contributions to the pressure according to Eqs. (10), (11), and (12) can be seen in Table III. While the volume term contributes rather largely to the pressure, in contrast to the situation of the internal energy the term P_{i-i}', coming from the derivative of $u(r;\rho)$ with

TABLE III. Contributions to the pressure P according to Eqs. (10), (11), and (12).

	$\beta P_{id}/\rho$	$\beta P_0/\rho$	$\beta P_{i-i}'/\rho$	$\beta P_{i-i}''/\rho$	$\beta P/\rho$
Li	1	−14.35	17.61	−0.30	3.96
Na	1	−20.85	15.49	0.52	−3.84
K	1	−24.97	11.97	0.14	−11.87
Rb	1	−28.08	12.03	−0.20	−15.25
CS	1	−28.78	10.01	−0.28	−18.05

TABLE IV. Contributions to the bulk modulus $\beta(\partial P/\partial\rho)_T$ according to Eq. (26), which has been fitted to the experimental values of (a). Ruppersberg and Speicher (Ref. 31) and (b) Webber and Stephens (Ref. 32).

	$\beta P''_{i-i}/\rho-1$	B_1	B_2	B_3	B_4	$\beta\rho^2[\partial^2 U_0(\rho)/\partial\rho^2]$	$\beta(\partial P/\partial\rho)_T=1/S_{\exp}(0)$
Li	−1.31	−8.68	5.44	39.29	−5.34	9.06	38.46[a]
Na	−0.48	−9.29	4.89	42.87	−1.85	7.42	43.56[b]
K	−0.86	−12.89	8.21	40.75	1.14	5.31	41.66[b]
Rb	−1.20	−16.32	11.72	43.35	2.82	5.08	45.45[b]
Cs	−1.28	−18.57	12.35	42.49	2.31	4.36	41.66[b]

respect to r, is comparable to P_0 with the opposite sign. The term P''_{i-i} taking account of the density dependence of the pair potential is very small compared to P_0.

An expression for $\beta(\partial P/\partial\rho)|_T$ may also be obtained, which reduces to that of simple liquids when the density of $u(r;\rho)$ is dropped:

$$\beta\frac{\partial P}{\partial\rho}\bigg|_T=2\frac{\beta P}{\rho}-1+\frac{\beta P''_{i-i}}{\rho}+\beta\rho^2\frac{\partial^2 U_0(\rho)}{\partial\rho^2}+\sum_{p=1}^{4}B_p\ , \tag{26}$$

where P and P''_{i-i} are those of Eqs. (9) and (12), respectively. The other four terms, B_p are defined as

$$B_1=-2\pi\beta\rho\int r^2 g(r;\rho)\frac{r\rho}{3}\frac{\partial^2 u(r;\rho)}{\partial\rho\partial r}dr\ , \tag{27}$$

$$B_2=2\pi\beta\rho\int r^2 g(r;\rho)\rho^2\frac{\partial^2 u(r;\rho)}{\partial\rho^2}dr\ , \tag{28}$$

$$B_3=-2\pi\beta\rho^2\int r^2\frac{\partial g(r;\rho)}{\partial\rho}\frac{r}{3}\frac{\partial u(r;\rho)}{\partial r}dr\ , \tag{29}$$

$$B_4=2\pi\beta\rho^2\int r^2\frac{\partial g(r;\rho)}{\partial\rho}\rho\frac{\partial u(r;\rho)}{\partial\rho}dr\ . \tag{30}$$

Table IV shows the individual contributions of $\beta(\partial P/\partial\rho)_T$. While the volume term $U_0(\rho)$ is crucial for describing energy and pressure of liquid metals, it can be ignored, as well as the density dependence of the pair potential when the bulk modulus is calculated. It is found that $\beta(\partial P/\partial\rho)_T$ can be determined with a good degree of accuracy in considering the assumption that the pair potential is independent of the density, with the term B_3 only. This fact as been previously pointed out by Finnis[24] in calculating the elastic constants in the solid state, from the effective interionic potential

IV. CONCLUSION

We have presented the results of the structure of the alkali metals by using the HMSA, which combines both the integral equation, and the thermodynamic perturbation theories. Comparison of our results with the experimental data of $S(q)$ establishes the validity of the HMSA for direct application to fluids with continuous effective pair potentials. It clearly demonstrates that our self-consistency procedure, based on a conjointed study of structure and thermodynamics, provides very good results, as much for the structure factor as for the thermodynamic properties.

We also have examined the influence of the parameters of the pseudopotential, and the local-field correction on the structure. Concerning the influence of the tail of the pair potential and the cutoff distance, we found that the presence of long-range attractive part of $u(r)$ enhances the oscillations of $g(r)$ and $S(q)$ but does not modify their location. The knowledge of all these behaviors has been helpful to set up the HMSA procedure.

We are presently performing the calculations of the structure of liquid transition metals with the HMSA, for which a theoretical pair potential has been recently obtained (Bretonnet, Bhuiyan, and Silbert[38]). The results, which will be published shortly, are very encouraging, therefore we have planned to apply the inversion technique, allowing extraction of the pair interaction from the structural data, to test the resulting effective pair potential for transition metals.

[1]R. Kumaravadivel and R. Evans, J. Phys. C **9**, 3877 (1976).
[2]I. L. McLaughlin and W. H. Young, J. Phys. F **12**, 245 (1982).
[3]G. Kahl and J. Hafner, Phys. Rev. A **29**, 3310 (1984).
[4]J. L. Bretonnet and C. Regnaut, Phys. Rev. B **31**, 5071 (1985).
[5]Y. Rosenfeld and N. H. Ashcroft, Phys. Rev. A **20**, 1208 (1979).
[6]N. Matsuda, H. Mori, K. Hoshino, and M. Watabe, J. Phys. Condens. Matter **3**, 827 (1991).
[7]L. E. Gonzalez, D. J. Gonzalez, and M. Silbert, Physica B **168**, 39 (1991).
[8]H. C. Chen and S. K. Lai, Phys. Rev. A **45**, 3831 (1992).
[9]F. J. Rogers and D. A. Young, Phys. Rev. A **30**, 999 (1984).
[10]G. Zerah and J. P. Hansen, J. Chem. Phys. **84**, 2336 (1986).
[11]G. Kahl, Phys. Rev. A **43**, 822 (1991).
[12]W. G. Madden and S. A. Rice, J. Chem. Phys. **72**, 4208 (1980).
[13]N. Jakse and J. L. Bretonnet, J. Non-Cryst. Solids **156-158**, 149 (1993).
[14]P. Vashishta and K. S. Singwi, Phys. Rev. B **6**, 875 (1972).
[15]S. Ichimaru and K. Utsumi, Phys. Rev. B **24**, 7385 (1981).
[16]K. Hoshino and W. H. Young, J. Phys. F **16**, 1659 (1986).
[17]T. Das and R. N. Joarder, J. Non-Cryst. Solids **117-118**, 583 (1990).
[18]M. Hasegawa, K. Hoshino, M. Watabe, and W. H. Young, J. Non-Cryst. Solids **117-118**, 300 (1990).
[19]D. Weeks D. Chandler, and H. C. Anderson, J. Chem. Phys. **54**, 4931 (1970).
[20]S. K. Lai, L. Wang, and M. P. Tosi, Phys. Rev. A **42**, 7289 (1990).

[21]J. L. Bretonnet and N. Jakse, Phys. Rev. B **46**, 5717 (1992).
[22]P. A. Egelstaf, *An Introduction to the Liquid State* (Academic, New York, 1967).
[23]M. Hasegawa and M. Watabe, J. Phys. Soc. Jpn. **32**, 14 (1972).
[24]M. W. Finnis, J. Phys. F **4**, 1645 (1974).
[25]E. G. Brovman and Y. Kagan, Zh. Eksp. Teor. Fiz. **57**, 1329 (1969) [Sov. Phys. JETP **30**, 721 (1970)].
[26]M. J. Gillan, Mol. Phys. **38**, 1781 (1979).
[27]S. Labik, A. Malijevsky, and P. Vonka, Mol. Phys. **56**, 709 (1985).
[28]M. J. Huijben and W. van der Lugt, Acta Crystallogr. Sect. A **35**, 431 (1979).
[29]J. R. D. Copley and J. M. Rowe, Phys. Rev. A **9**, 1656 (1974).
[30]Y. Waseda, *The Structure of Non-Crystalline Materials* (McGraw-Hill, New York, 1980).
[31]H. Ruppersberg and W. Speicher, Z. Naturforsch. **31a**, 47 (1976).
[32]G. M. B. Webber and R. W. B. Stephens, *Physical Acoustics 4B* (Academic, New York, 1968).
[33]J. Chihara, Prog. Theor. Phys. **50**, 1156 (1973).
[34]G. Franz, W. Freyland, W. Gläser, F. Hensel, and E. Schneider, J. Phys. (Paris) Colloq. **41**, C8-70 (1980).
[35]R. Winter, F. Hensel, T. Bodensteiner, and W. Gläser, Ber. Bunsenges. Phys. Chem. **91**, 1327 (1987)
[36]N. Matsuda, K. Hoshino, and M. Watabe, J. Chem. Phys. **93**, 7350 (1990).
[37]K. A. Gschneidner, in *Solid State Physics: Advances in Research and Applications,* edited by F. Seitz and D. Turnbull (Academic, New York, 1964), Vol. 16, p. 275.
[38]J. L. Bretonnet, G. M. Bhuiyan, and M. Silbert, J. Phys. Condens. Matter **4**, 5359 (1992).